SLAC – PUB – 3619
April 1985
(A)

THE DESIGN AND PERFORMANCE OF A 150 MW KLYSTRON AT S-BAND*

T. G. LEE, G. T. KONRAD, Y. OKAZAKI,†
M. WATANABE,* H. YONEZAWA†
Stanford Linear Accelerator Center
Stanford University, Stanford, Califoria, 94305

ABSTRACT

Design considerations and performance characteristics of a 150 MW pulsed klystron amplifier at S-Band are described. One of the main problems encountered in generating such high power at microwave frequencies is the extremely high voltage gradients developed across the output gap of the klystron which may cause RF breakdown. A double-gap 2π-mode output cavity is used successfully in the present case to generate a peak output power of 150 MW at a frequency of 2870 MHz with an efficiency of 51%, saturation gain of 59.3 dB and a pulse width of one microsecond. A reduction in gap voltage of at least 25% as compared to a similar klystron with a conventional single-gap output cavity at the same voltage and at their respective maximum efficiency points is theoretically predicted. Examination of the gaps after an extended period of operation shows that they are smooth and without signs of erosion, indicating that the fields were uniform and not excessive. Extrapolating from the gradient which exists in this present tube, it appears feasible to generate still higher powers (of the order of 700 MW) efficiently with a single klystron at S-Band with a pulse width of one microsecond, if the need arises.

Submitted to *IEEE Transactions on Plasma Science on High-Power Microwave Generation*

* Work supported by the Department of Energy, contract DE – AC03 – 76SF00515.
† Currently at Toshiba Corporation, Kawasaki, Japan
* Currently at Mitsubishi Electric Corporation, Tokyo, Japan

1. Introduction

The multi-cavity klystron amplifier is a well-established device and has a good record of achievement in efficiently generating large amounts of CW and pulsed powers at microwave frequencies. The ever-increasing demand for more power (hundreds of megawatts per tube) for contemplated new particle accelerators has given the klystron a new challenge to show its versatility. The following is a description of the development of a klystron producing a peak output power of 150 MW with an efficiency of 51% and a saturation gain of 59.3 dB at S-Band.

2. Design Considerations

2.1 Electron Gun

The electron gun is a simple Pierce-type solid beam gun designed with the SLAC Electron Trajectory Program to operate at a voltage between 450 and 500 kV with a microperveance of 2.0. The radii of the focus electrode and the anode electrode are made rather large in order to minimize the gradient. Some pertinent parameters are as follows:

Design voltage	450 kV
Beam current	603 A
Pulse width	1 μsec
Uniformity of cathode loading (from edge to center)	1.44 to 1
Maximum cathode loading	8.24 A/cm^2
Maximum electric field (on anode surface)	222 kV/cm
Maximum electric field (on cathode surface)	208 kV/cm
Cathode radius	5.26 cm
Area convergence ratio	16 to 1
Type of emitter	oxide-coated

The voltage-current operating characteristics of the gun are shown in Fig. 1. It is seen that the microperveance at 200 kV is slightly above 2.0 but falls to 1.92

at a voltage of 450 kV, a little short of the design value of 2.0. The reduction in perveance can be explained in part by relativistic effects. The approximate relativistic correction factor for perveance is:[1]

$$k = 1 - (0.107)\frac{V}{V_n} + (0.024)\left(\frac{V}{V_n}\right)^2 - \ldots \qquad (1)$$

where

$$\frac{V}{V_n} = \frac{V(\text{in kV})}{511} \quad .$$

According to the above correction factor, the drop in perveance should be 3.9% when the voltage is raised from 200 kV to 450 kV. The actual drop, however, was 7%. The additional decrease may be due to non-uniformity of cathode emission or measurement errors attributed to non-ideal current pulse waveform. Except for the slightly lower than design perveance, the gun worked satisfactorily. There were no gun oscillations or serious arcing.

2.2 RF Cavities

The design of the bunching section is rather conventional and we will not discuss it at length except to say that it is comparatively long because of the highly relativistic velocities involved. A schematic drawing of the interaction region is shown in Fig. 2. The spacings of the four bunching cavities and their resonant frequencies were optimized by computer, using a one-dimensional disk model code. The output cavity, however, requires some special attention. A double-gap extended-interaction cavity is used to reduce the high fields expected. The main objective is to design an output circuit which has the lowest gap fields consistent with good efficiency and stability. The important parameters to be considered are listed below:

1. Choice of operating mode.
2. Optimum d.c. transit angle between gaps.

3. Optimum gap impedance amplitude and phase angle.

4. Optimum distance between output cavity and penultimate cavity.

5. Stability.

When two cavities are coupled inductively through slots in the common wall, the modes which are of greatest concern to us are the π-mode and the 2π-mode. In dealing with very high powers, the choice of which mode to use for amplification is important for reasons of field uniformity. In the early stages of this development program we had used a π-mode two-gap output cavity operating at a voltage of 270 kV (40 MW output power level) and encountered serious problems with output gap erosion due to asymmetry in the azimuthal direction of the longitudinal electric field caused by the coupling slot. The electric field was always higher on the side of the slot (as much as 2:1) with the result that the beam was deflected, hit one side of the noses of the cavity, and seriously damaged them. Of course, this serious non-uniformity of the gap fields nullifies the potential advantages of a multiple-gap cavity. The explanation for this field distortion can be found in the fact that in the π-mode there is a net current flowing into the slot.[2] In the 2π-mode, on the other hand, there is no net current flow into the slot and the fields are more uniform. This has been verified both in cold test and in the actual operating klystron using a 2π-mode double-gap output cavity at the 150 MW level. For extremely high powers, it is therefore desirable to choose the 2π-mode for amplification.

The critical parameters listed above in points 1, 2 and 3 have been studied with a computer program to be described below which can handle multiple-gap cavities as well as conventional single-gap cavities. The output gap voltages are calculated by the following relation:

$$\begin{pmatrix} V_1 \\ V_2 \end{pmatrix} = \begin{pmatrix} Z_{11} & Z_{12} \\ Z_{21} & Z_{22} \end{pmatrix} \begin{pmatrix} I_1 \\ I_2 \end{pmatrix} \tag{2}$$

where Z_{ij} are the complex gap impedances of the output cavity which can be measured by cold test methods and I_1 and I_2 are the induced currents in each

gap. So, a set of physically realizable output impedance matrix parameters can be input into the program to study tube performance. Computer results indicate that optimum efficiency is obtained when the d.c. transit angle between gaps falls near the point of maximum negative beam-loading conductance (see Fig. 3). The beam coupling coefficient and the beam-loading conductance of the output cavity used are shown in Figs. 4 and 5. This optimum transit angle between gaps corresponds to about 280 degrees at 450 kV.

The optimum values of gap impedance amplitude and phase as calculated are shown in Figs. 6 and 7, based on the assumption of equal $|\varsigma_{ij}|$'s and $\phi_{22} = \phi_{12} = \phi_{21} = 0$. We found that an impedance amplitude of between 500 and 600 ohms for both gaps gives the best efficiency and that the phase angles of the impedances should be close to zero degrees. When the phase angle of the impedance of the first gap, ϕ_{11}, deviates from zero, the efficiency starts to fall and the resulting gap voltages no longer remain equal to each other. In practice, it is difficult to make all the phase angles zero. If the second of the two coupled cavities (i.e., the downstream one with the output waveguide attached) is made resonant at the signal frequency, ϕ_{22}, ϕ_{12} and ϕ_{21} will be zero. The phase angle, ϕ_{11}, however, may not be zero, depending on the degree of coupling between the cavities and their relative resonance frequencies. In a conventional single-gap klystron, the output gap impedance can be obtained by separate measurements of R/Q and Q_{ext}, and the impedance is defined as the ratio of the voltage across the gap to the current by which the voltage is induced. In a two-gap cavity, the beam passes through two gaps sequentially and the ac components of current differ both in amplitude and phase. Moreover, the current will not only induce a voltage on the gap it passes but also induces a voltage on the other gap, so there are at least three impedances which we have to deal with (i.e., Z_{11}, Z_{22} and Z_{12} which is the same as Z_{21} due to reciprocity). A method of measuring these impedances has been developed by Zhao,[3] who used a three-port microwave network to represent the system. One of the ports is the output waveguide and the other two represent the two gaps of the cavity. An impedance matrix is used

to characterize the system and the six independent impedance parameters can be found by measuring the input impedance seen from the output waveguide when the two gaps are in different conditions, viz., either open, shorted, or perturbed with an added capacitance. The gap impedance matrix measured this way at a frequency of 2870 MHz for the double-gap output cavity used is as follows:

$$Z_{ij} = \mid \varsigma_{ij} \mid e^{j\phi_{ij}} \qquad , \qquad i,j = 1,\, 2$$

$$\varsigma_{11} = 457\Omega,\ \phi_{11} = 16^\circ$$

$$\varsigma_{22} = 565\Omega,\ \phi_{22} = -18^\circ$$

$$\varsigma_{21} = \varsigma_{12} = 510\Omega,\ \phi_{12} = \phi_{21} = -18^\circ$$

These impedance values are near, though not exactly equal, to the optimum values calculated by the computer program.

The optimum distance between the middle of the first gap of the output cavity and the penultimate cavity has a rather broad range between 20° and 40° of a reduced plasma wavelength as indicated in Fig. 8. Twenty-four degrees was actually chosen.

It is well-known that tubes with multiple-gap cavities are subject to the possibility of self-oscillation because of the existence of a region of negative beam-loading conductance. For stability in that region of operation, it is necessary that the absolute value of beam-loading conductance be less than the circuit conductance for both modes of the circuit. The frequencies of the various modes are shown in Fig. 9, which was obtained with a swept frequency source. At the 2π-mode, the maximum negative normalized beam-loading conductance is -0.29 (see Fig. 5), which is less than the measured circuit conductance and should not (in fact, did not) lead to self-oscillations. At the π-mode frequency of 2472 MHz the calculated normalized beam-loading conductance is $+0.388$ and there is no danger of self-oscillation there, in spite of the fact that the Q is rather high. The slot mode resonates at 3445 MHz which is very close to the frequency at which the two narrow coupling slots are 1/2 wavelength long. For the slot mode, the

measured axial electric field in one gap is very much weaker than the other and stability is not a problem.

3. Experimental Results

3.1 General Test Results

Figure 10 shows the power output, saturation gain, and efficiency versus beam voltage at a signal frequency of 2870 MHz (the performance at 2870 MHz is slightly better than at 2856 MHz; data elsewhere in this paper refer to 2856 MHz). As indicated in the figure, the peak power output at 450 kV is 126 MW with an efficiency of 48.2% and a saturation gain of 57.3 dB. When the beam voltage was raised to 475 kV, the power output reached 150.4 MW with a corresponding efficiency of 51% and saturation gain of 59.3 dB. The pulse width was 1.0 μsec and the repetition rate 60 pps except for 465 kV, 470 kV, and 475 kV points where the pulse repetition rate was reduced to 40 pps due to modulator limitations.The repetition rate can be increased to 180 pps with correspondingly higher average power output if the beam voltage does not exceed 450 kV. The single output window, which is of the pill-box type with a 99.5% Al_2O_3 ceramic disk of 3.33 inch diameter and 0.125 inch thickness, is capable of handling the peak and average power generated in this tube without any difficulty. Beam pulse shapes and RF output pulse shapes at various voltages are shown in Fig. 11 and a transfer characteristic curve is shown in Fig. 12. The modulation seen on the beam voltage pulse in Fig. 11 is due to noise picked up by the capacitive voltage divider in the viewing circuit and is not inherent in the klystron. The tube operated stably as a function of drive level. Figure 13 shows RF pulse shapes at saturation drive, -2 dB below saturation drive and $+4.4$ dB above saturation drive at a voltage of 425 kV, 2870 MHz signal frequency. The tube operated for about 1000 hours, most of which were at a power level of 100 MW, before it was finally removed from test and cut open for examination. The purpose of opening up the tube was to observe the condition of the output gaps after

extended operation and to measure the output cavity gap impedance parameters more extensively. First of all, it was re-assuring to find that the output gaps were smooth and in good shape (no arc marks or erosion) after 1000 hours of operation, indicating that the RF fields in the output cavity were fairly uniform and not excessive. Recall that the reason we chose to design the cavity to operate at the 2π-mode rather than the π-mode was to avoid the non-uniformity of axial electric field in the azimuthal direction due to the presence of the coupling slot in the common wall. Experimental evidence proved that this choice was a correct one.

3.2 Comparison with Computation

The computer program which was developed in the course of this work[4] has been useful in the design of the klystrons, although it is a relatively simple one-dimensional, time-stepping disk model with space charge and relativistic effects taken into account. A comparison of the calculated results using the actually measured parameters of beam current, cavity frequencies, cavity spacings, gap impedance values, etc., with the experimentally measured results at 425 kV is shown in Fig. 12. The agreement in maximum efficiency attained is very good, while the discrepancy between calculated saturation gain and measured saturation gain is 1.5 dB.

3.3 Comparison with a Single-Gap Klystron of Similar Power Level

In the course of this work, we have also built a klystron with a conventional single-gap output cavity. The test results for this tube are shown in Fig. 14. Note that the efficiency obtained from the 2π-mode double-gap output tube is higher by 5 percentage points at 450 kV and by 8 percentage points at 475 kV. In addition, the RF voltage gradient across each gap in the two-gap cavity is lower than that of the single-gap output klystron. Although we have no easy

way of experimentally measuring the gap voltages in the output cavity during operation, our calculations indicate that a reduction of 25% in gap voltage is obtained at the maximum efficiency point. The calculated output gap voltages for the two-gap tube at 450 kV are shown in the computer printout in Fig. 15, and they are 367 kV and 373 kV respectively. A similar calculation for the single-gap case gives a gap voltage of 492 kV at the same operating voltage, but its efficiency is lower by about 4 percentage points. The reduction in gap voltage would be more than 25% if compared at the same power output level. This reduction in the voltage gradient across the gap is very important if one wishes to obtain even higher powers from a klystron, as for example in future particle accelerator applications. The distance versus time plot in the computer printout of Fig. 15 also shows the desired property that the first gap of the two-gap output cavity gives further bunching to the beam while extracting a portion of its energy and the second gap doing the remainder of the energy extraction. It should be pointed out, however, that this particular comparison is not meant to imply that a double-gap output klystron is, in general, superior in efficiency to a single ouput gap klystron. A single output gap tube can be made just as efficient if its design is properly optimized. Also, a single gap tube can probably generate 150 MW of peak power, although it would be close to the limit of permissible gap gradient. A double-gap output cavity klystron has shown that it can easily handle this level of power and offers the possibility of generating even more, if required.

4. Measurements of Harmonic Content of the RF Output

It is interesting to obtain some idea of the harmonic content of the output signal from a very high power klystron. Quantitative measurements have been made on the single-gap klystron reported above at a beam voltage of 450 kV by the multiple-probe method.[5] The method consists of placing four calibrated electric probes on the broad wall of the output waveguide at each of two different waveguide cross sections and one calibrated electric probe on the narrow wall at

each of four different waveguide cross sections to measure the electric field components of all the possible propagating modes at the second and third harmonic of the signal frequency for the size waveguide used and then feeding the measured data into a computer for final calculation of the harmonic contents. The multiple-probe assembly used and a block diagram of the test set-up are shown in Fig. 16. The results of this measurement are tabulated below.

As shown, the second harmonic is 32 dB below the fundamental and the third harmonic is about 39 dB below. These values are of the same order of magnitude as found in ordinary klystrons operating at lower voltage levels. Thus it appears that the basic mechanisms of klystron bunching are essentially the same up to the highly relativistic region of 450 kV.

Multimode Harmonic Power Output (Peak power in Watts)
150 MW Klystron No. 1 (saturation conditions)
Beam Voltage = 450 kV, Beam Current = 555 A

Propagating Mode	Fundamental (2856 MHz)	2nd Harmonic (5712 MHz)	3rd Harmonic (8568 MHz)
TE_{10}	108 E06 W	13,287 W	3,052 W
TE_{20}	Below Cutoff	48,648	400
TE_{01}	Below Cutoff	1,748	2,580
TE_{11}	Below Cutoff	960	3,082
TM_{11}	Below Cutoff	2,782	975
TE_{21}	Below Cutoff	Below Cutoff	74
TM_{21}	Below Cutoff	Below Cutoff	790
TE_{30}	Below Cutoff	Below Cutoff	1,407
TE_{31}	Below Cutoff	Below Cutoff	761
TM_{31}	Below Cutoff	Below Cutoff	906
TE_{40}	Below Cutoff	Below Cutoff	360
Total	108 E06 W (0 dB, Ref.)	67,425 W (-32.0 dB)	14,387 W (-38.75 dB)

5. Conclusions

The concept of multiple-gap or extended interaction cavities is not new.[6-9] The significance of this work is that it applied this concept successfully to a new level of power output and provided a viable option for the generation of even higher powers at microwave frequencies. The average gradient across each output gap at 450 kV in this development is only 177 kV/cm and the calculated maximum field is 275 kV/cm. A gradient at least twice this value at one microsecond pulse width should be feasible, based on work done at SLAC on high gradient accelerator structures. Hence, peak powers of the order of 700 MW could be generated at S-Band with one microsecond pulse width from a single klystron if the need arises.

Acknowledgments

This work was part of the agreement on "Cooperation in Research and Development in Energy and Related Fields" between the U.S. Government and Japan. The work was performed at Stanford Linear Accelerator Center with partial support from KEK Laboratory for High Energy Physics, Toshiba Corporation and Mitsubishi Electric Company. Helpful discussions with Dr. M. A. Allen and Dr. Marvin Chodorow are gratefully acknowledged.

References

1. W. A. Harman, *Fundamentals of Electronic Motion*, McGraw Hill, 1953, p. 297.

2. M. A. Allen, "Coupling of Multiple-Cavity Systems," Report No. 584, Microwave Laboratory, Stanford University, Stanford, CA, April 1959.

3. Y. X. Zhao, "An Impedance Measurement Method for Double-Gap Klystron Cavity," IEEE Trans. on Electron Devices, Vol. ED-29, No. 2, February 1982.

4. H. Yonezawa and Y. Okazaki, "A One-Dimensional Disk Model Simulation for Klystron Design," SLAC-TN-84-5, Stanford Linear Accelerator Center, Stanford, CA, May 1984.

5. W. R. Fowkes and E. S. Wu, "Multimode Harmonic Measurement of 40 MW Pulsed S-Band Klystrons," Conference on Precision Electromagnetic Measurements, CPEM 84, Delft, The Netherlands, Aug. 20-24, 1984.

6. T. Wessel-Berg, "A General Theory of Klystrons with Arbitrary Extended Fields," Report No. 376, Microwave Laboratory, Stanford University, Stanford, CA, 1957.

7. M. Chodorow and T. Wessel-Berg, "A High Efficiency Klystron with Distributed Interaction," IRE Trans. on Electron Devices, Vol. ED-8, pp. 44-55, January, 1961.

8. D. H. Preist and W. J. Leidigh, "Experiments with High-Power CW Klystrons Using Extended Interaction Catchers," IEEE Trans. on Electron Devices, Vol. ED-10, No. 5, pp. 201-211, May 1963.

9. J. Mann and D. Robinson, "X-Band Generator Development," RADC-TR-69-388, Final Technical Report, March 1970.

Figure Captions

1. Electron gun characteristics.
2. Electrical parameters, 150 MW klystron.
3. Calculated efficiency versus transit angle between gaps, 2π-mode double-gap output cavity.
4. Square of beam coupling coefficient versus beam voltage, 2π-mode double-gap output cavity.
5. Calculated beam-loading conductance versus $\beta_e p$, 2π-mode output cavity with space charge.
6. Calculated efficiency and gap voltage versus gap impedance, 2π-mode double-gap output cavity.
7. Calculated efficiency and gap voltage versus phase angle ϕ_{11}, 2π-mode double-gap output cavity.
8. Calculated efficiency versus distance between penultimate cavity and middle of first gap of double-gap output cavity.
9. Mode spectrum, double-gap output cavity.
10. Measured performance, 150 MW klystron with double-gap 2π-mode output cavity.
11. Beam pulse and RF pulse shapes at various voltages.
12. Measured performance and comparison with computation, at 425 kV beam voltage.
13. RF output pulse shapes at various levels of drive.
14. Measured performance, single-gap output klystron.
15. Computer printout of tube characteristics, 450 kV beam voltage.
16. Multiple-probe method of harmonic content measurement.

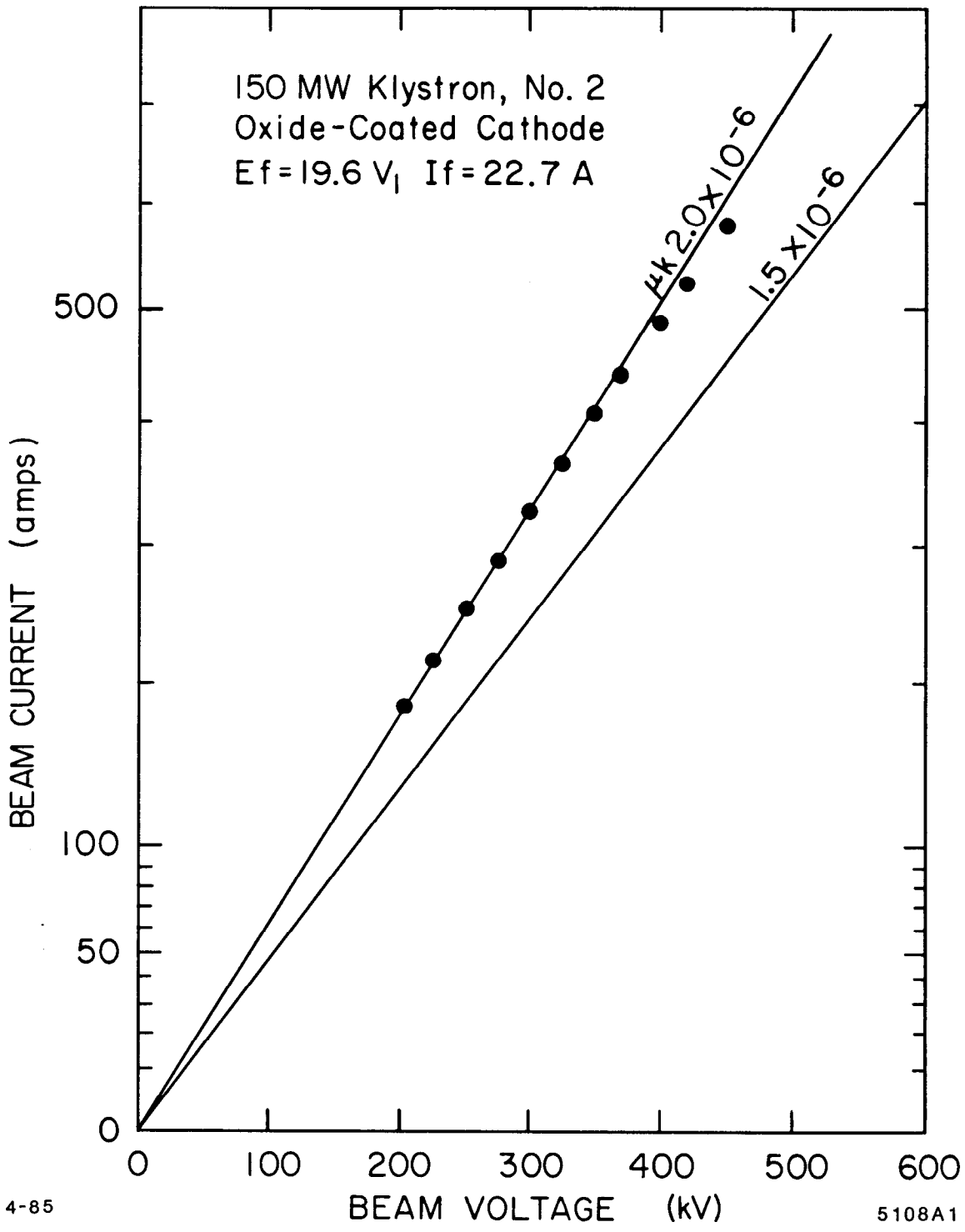
150 MW Klystron, No. 2
Oxide-Coated Cathode
Ef = 19.6 V, If = 22.7 A
μk 2.0 x 10-6
1.5 x 10-6
BEAM CURRENT (amps)
0
50
100
500
0
100
200
300
400
500
600
BEAM VOLTAGE (kV)
4-85
5108A1

Fig. 1

$V_0 = 450$ kV

$I_0 = 603$ A

$f_0 = 2856$ MHz

Perveance $= 2.0 \times 10^{-6} A/V^{3/2}$

$\gamma a = 0.708$

$\gamma b = 0.496$

Brillouin Focus Field = 598 Gauss

$\lambda q = 1.763$ m (calculated for partially shielded flow)

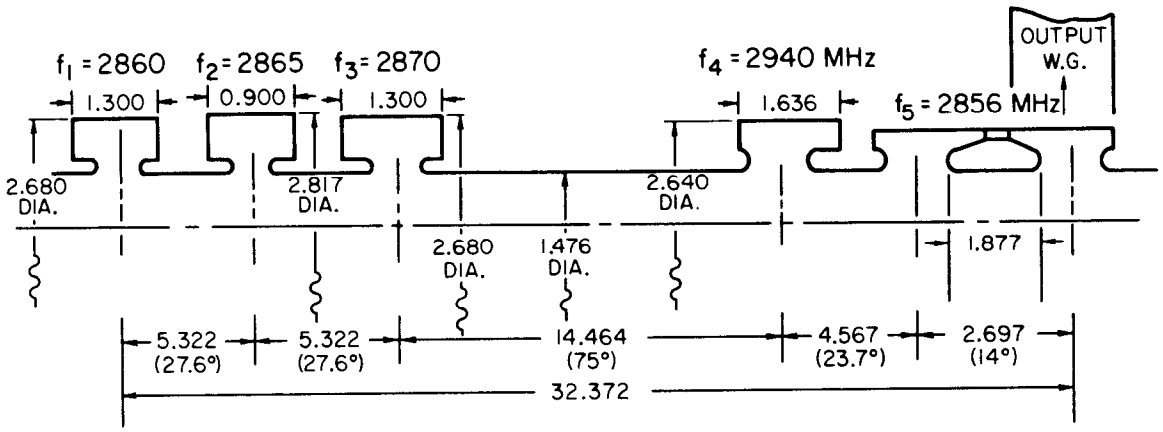

Note : Dimensions are in inches.
(not drawn to scale)

5-85

5108A2

Fig. 2

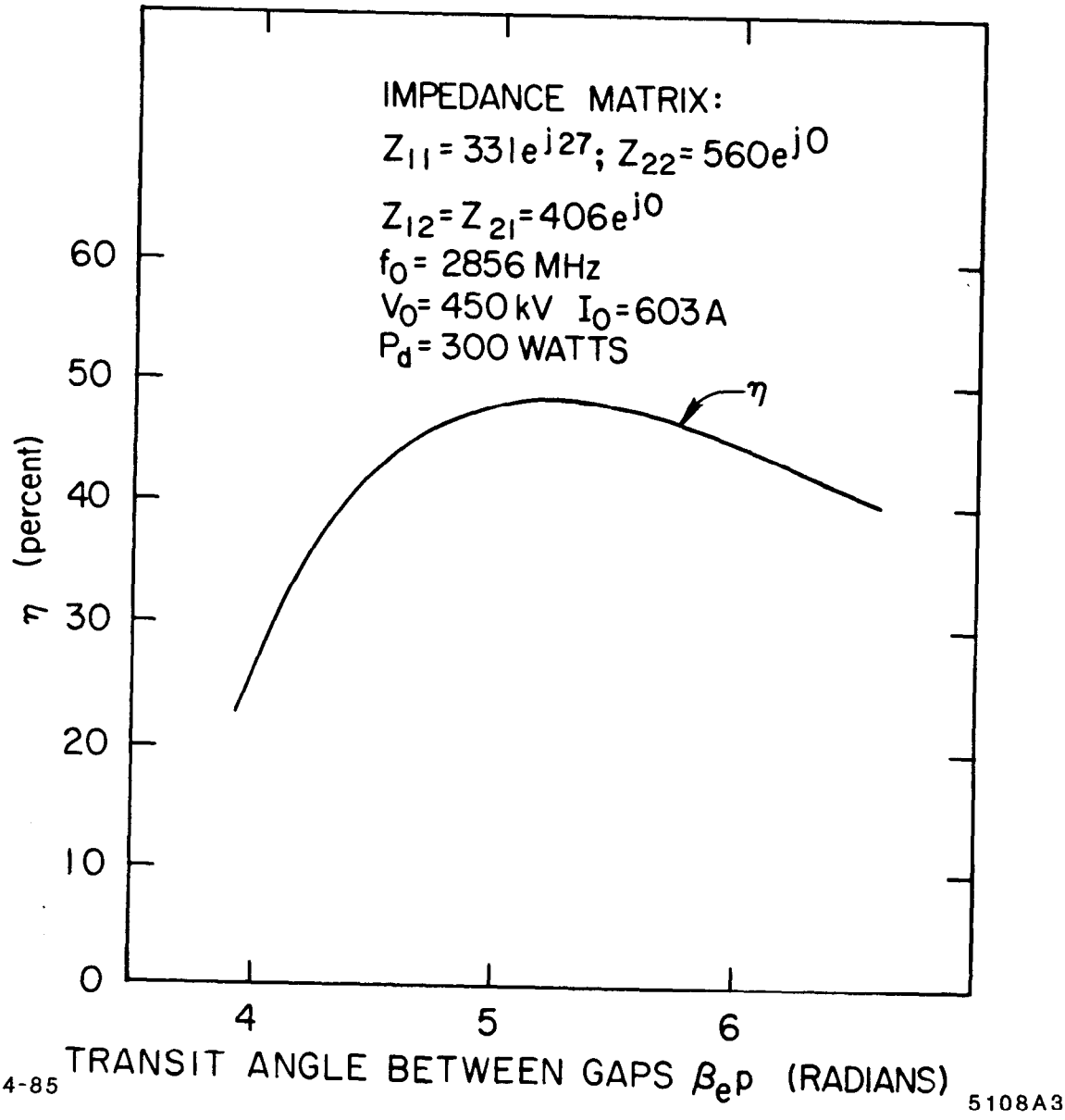
IMPEDANCE MATRIX:
$Z_{11} = 331e^{j27}$; $Z_{22} = 560e^{j0}$
$Z_{12} = Z_{21} = 406e^{j0}$
f_0 = 2856 MHz
V_0 = 450 kV I_0 = 603 A
P_d = 300 WATTS
η
η (percent)
60
50
40
30
20
10
0
4
5
6
TRANSIT ANGLE BETWEEN GAPS $\beta_e p$ (RADIANS)
4-85
5108A3

Fig. 3

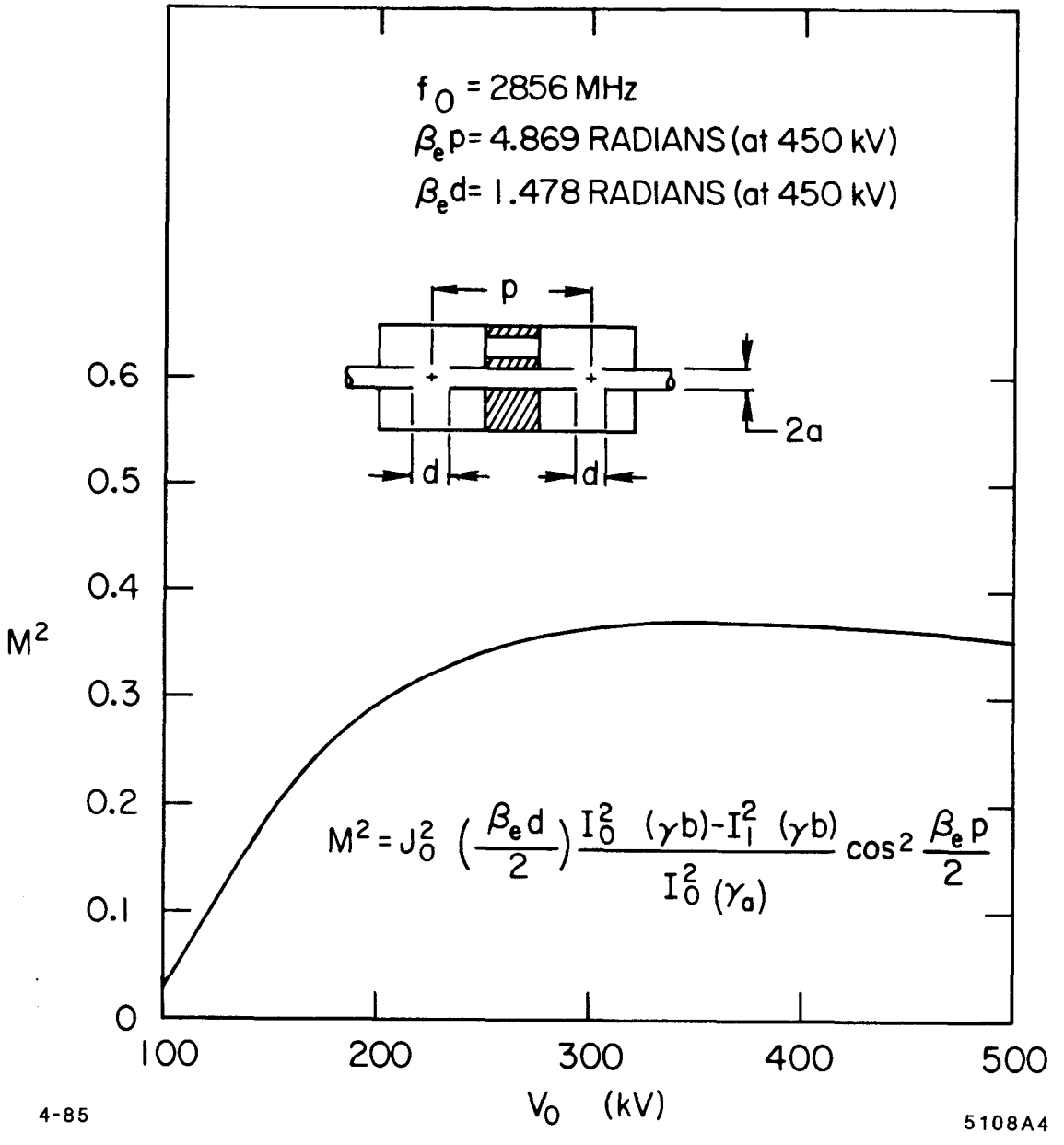
f_0 = 2856 MHz
$\beta_e p$= 4.869 RADIANS (at 450 kV)
$\beta_e d$= 1.478 RADIANS (at 450 kV)
p
2a
d
d
0.6
0.5
0.4
0.3
0.2
0.1
0
M^2
$M^2 = J_0^2 \left(\frac{\beta_e d}{2}\right) \frac{I_0^2(\gamma b) - I_1^2(\gamma b)}{I_0^2(\gamma_a)} \cos^2 \frac{\beta_e p}{2}$
100
200
300
400
500
V_0 (kV)
4-85
5108A4

Fig. 4

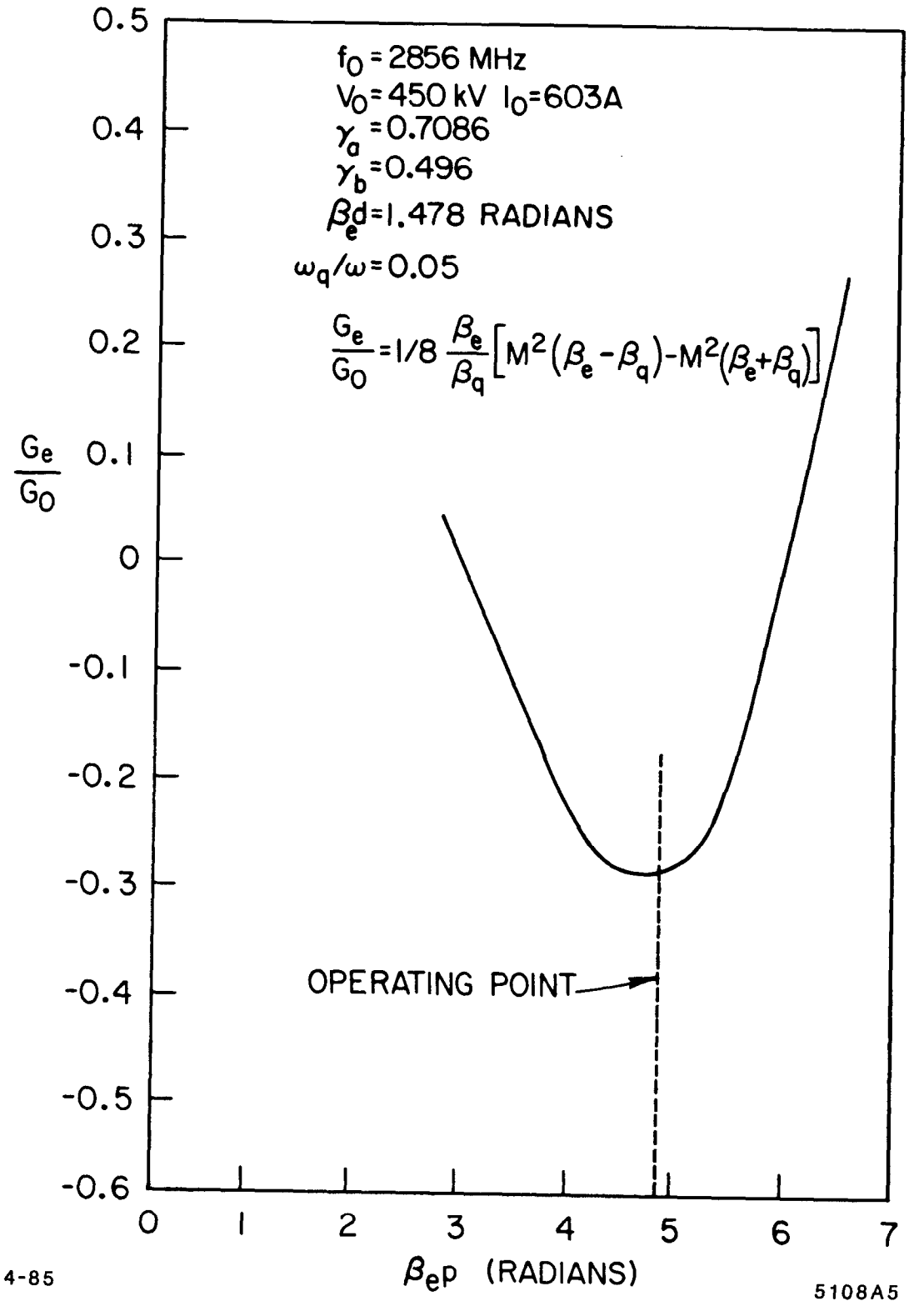
f_0 = 2856 MHz
V_0 = 450 kV I_0 = 603A
γ_a = 0.7086
γ_b = 0.496
$\beta_e d$ = 1.478 RADIANS
ω_q/ω = 0.05
$\frac{G_e}{G_0} = 1/8 \frac{\beta_e}{\beta_q}\left[M^2(\beta_e - \beta_q) - M^2(\beta_e + \beta_q)\right]$
$\frac{G_e}{G_0}$
0.5
0.4
0.3
0.2
0.1
0
-0.1
-0.2
-0.3
-0.4
-0.5
-0.6
OPERATING POINT
0
1
2
3
4
5
6
7
β_{ep} (RADIANS)
4-85
5108A5

Fig. 5

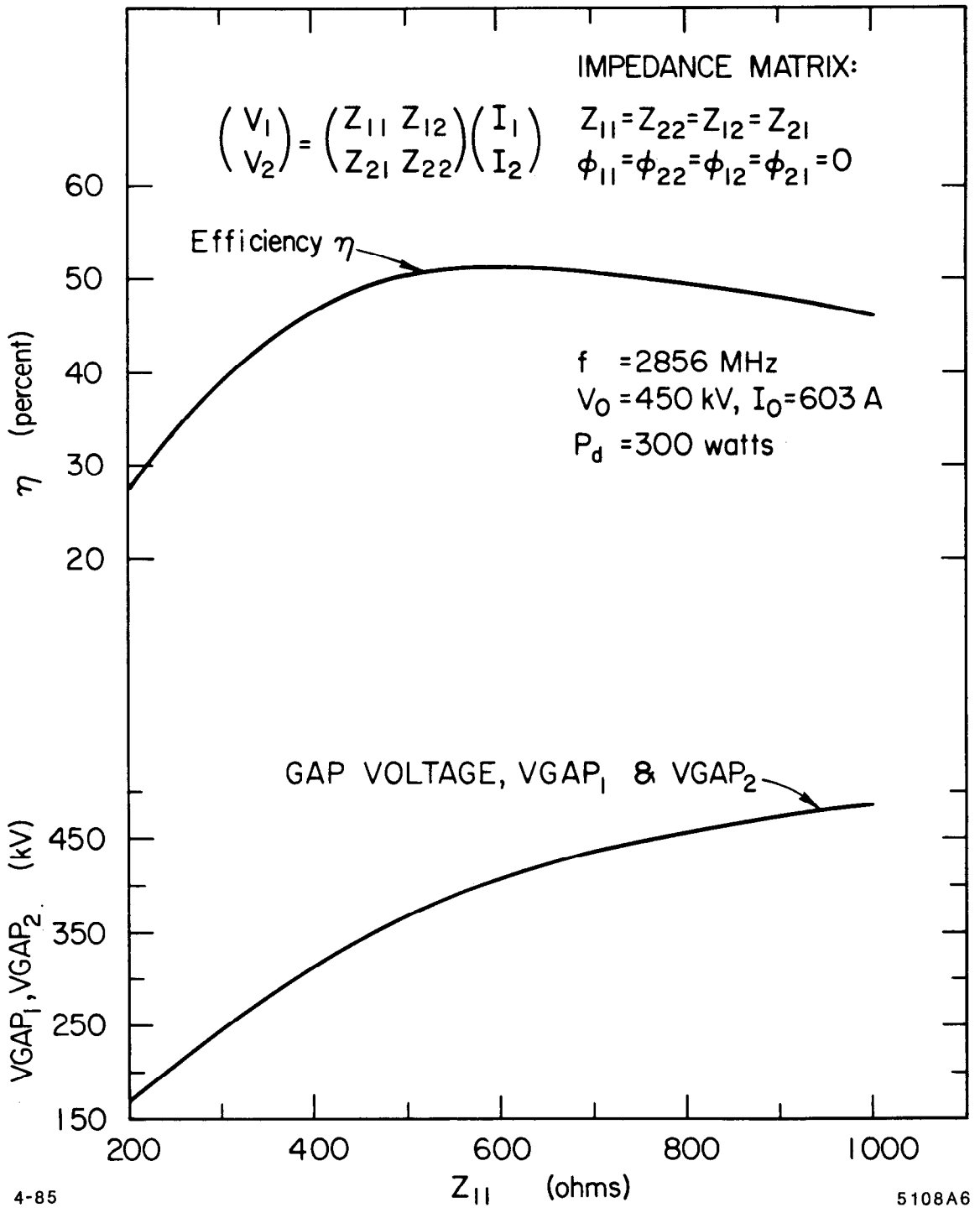
IMPEDANCE MATRIX:
$\begin{pmatrix} V_1 \\ V_2 \end{pmatrix} = \begin{pmatrix} Z_{11} & Z_{12} \\ Z_{21} & Z_{22} \end{pmatrix} \begin{pmatrix} I_1 \\ I_2 \end{pmatrix}$
$Z_{11}=Z_{22}=Z_{12}=Z_{21}$
$\phi_{11}=\phi_{22}=\phi_{12}=\phi_{21}=0$
Efficiency η
f =2856 MHz
V_0 =450 kV, I_0=603 A
P_d =300 watts
GAP VOLTAGE, $VGAP_1$ & $VGAP_2$
η (percent)
60
50
40
30
20
$VGAP_1, VGAP_2$ (kV)
450
350
250
150
200
400
600
800
1000
Z_{11} (ohms)
4-85
5108A6

Fig. 6

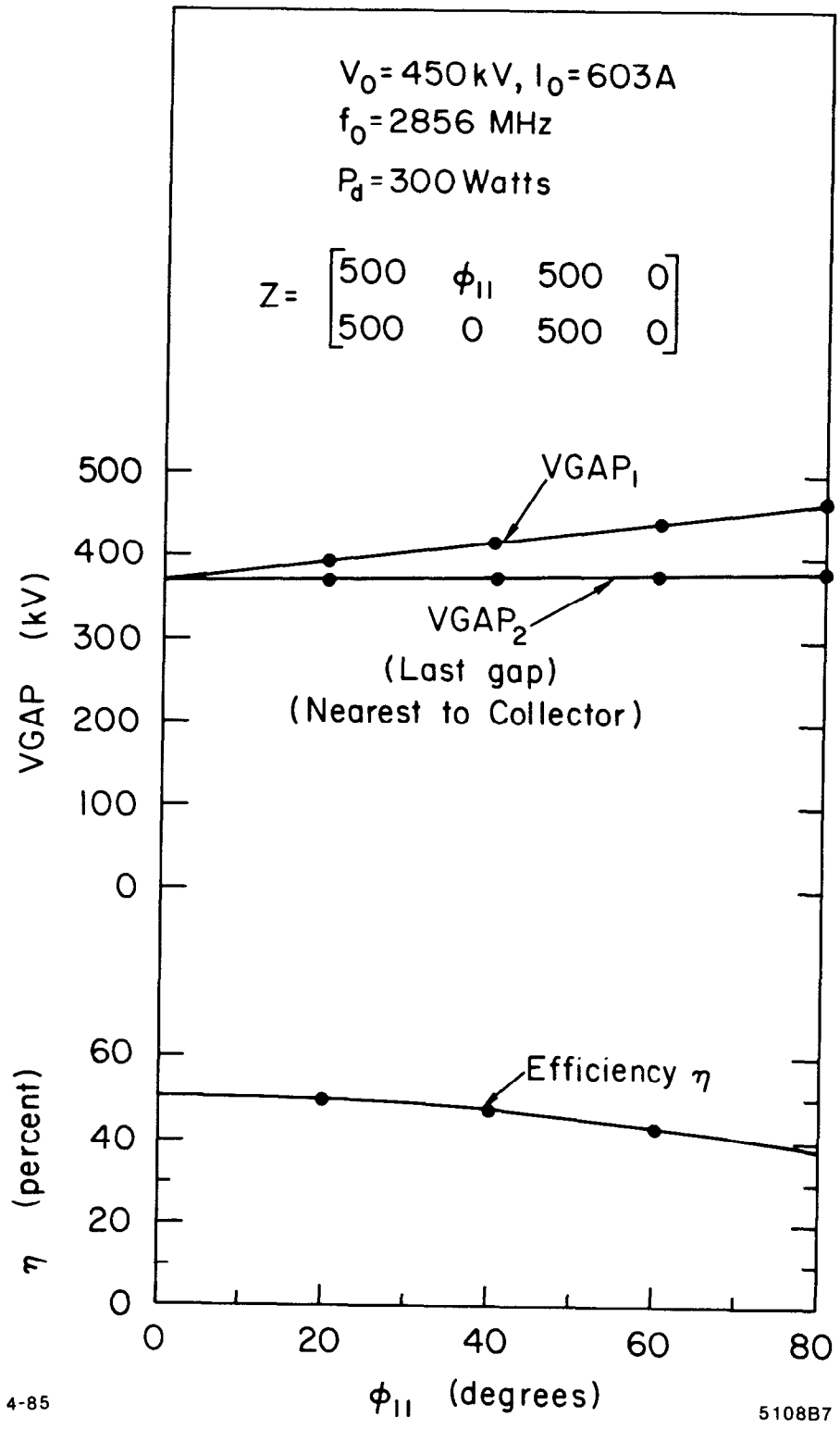
V_0 = 450 kV, I_0 = 603A
f_0 = 2856 MHz
P_d = 300 Watts
$Z = \begin{bmatrix} 500 & \phi_{11} & 500 & 0 \\ 500 & 0 & 500 & 0 \end{bmatrix}$
VGAP (kV)
500
400
300
200
100
0
$VGAP_1$
$VGAP_2$
(Last gap)
(Nearest to Collector)
η (percent)
60
40
20
0
Efficiency η
0
20
40
60
80
ϕ_{11} (degrees)
4-85
5108B7

Fig. 7

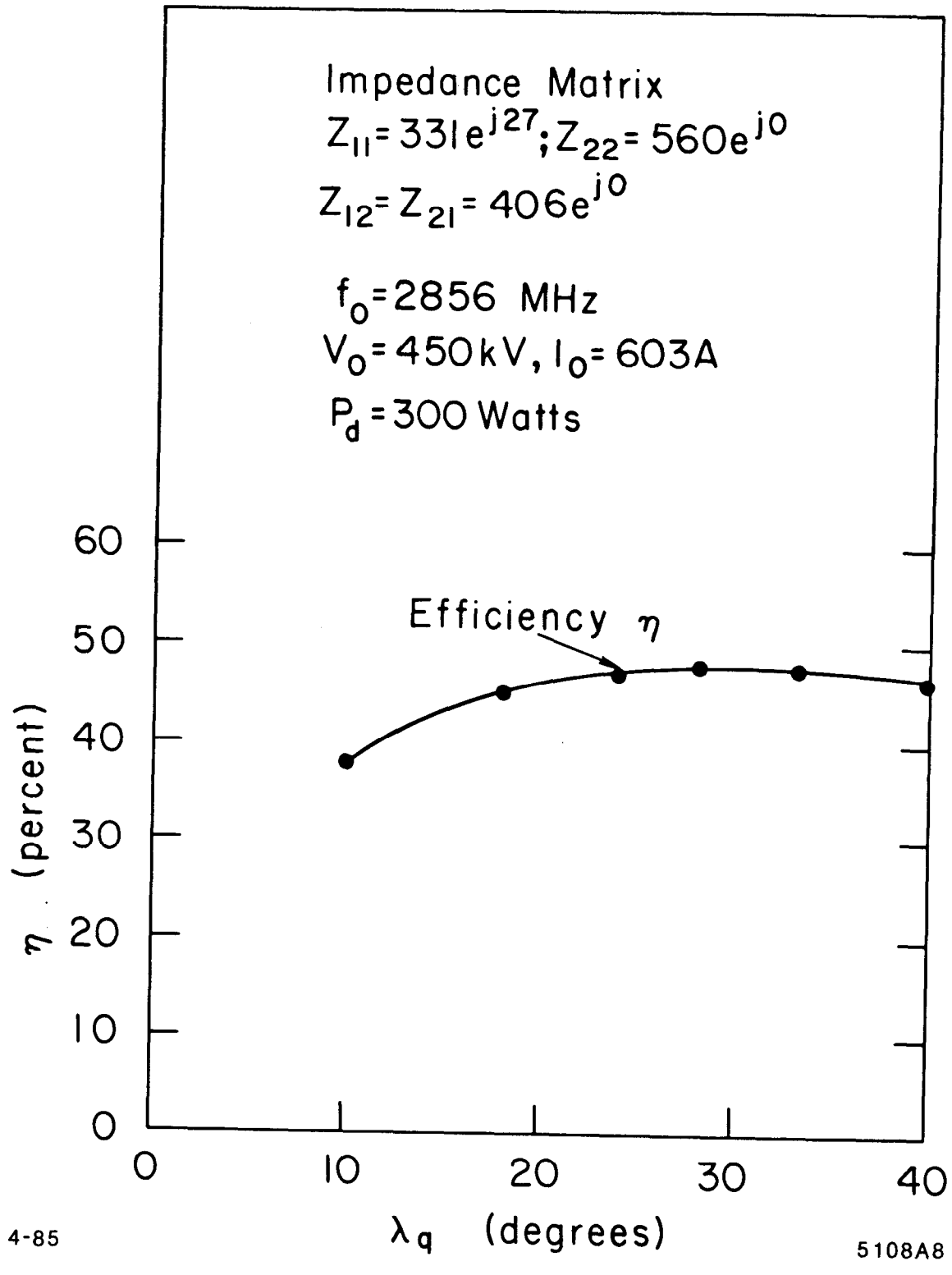
Impedance Matrix
$Z_{11}=331e^{j27}; Z_{22}=560e^{j0}$
$Z_{12}=Z_{21}=406e^{j0}$
$f_0=2856$ MHz
$V_0=450$kV, $I_0=603$A
$P_d=300$ Watts
Efficiency η
η (percent)
60
50
40
30
20
10
0
0
10
20
30
40
λ_q (degrees)
4-85
5108A8

Fig. 8

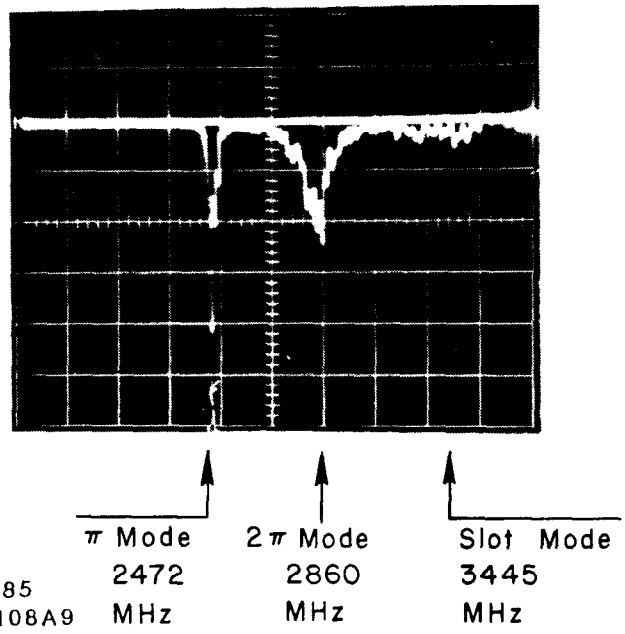

Fig. 9

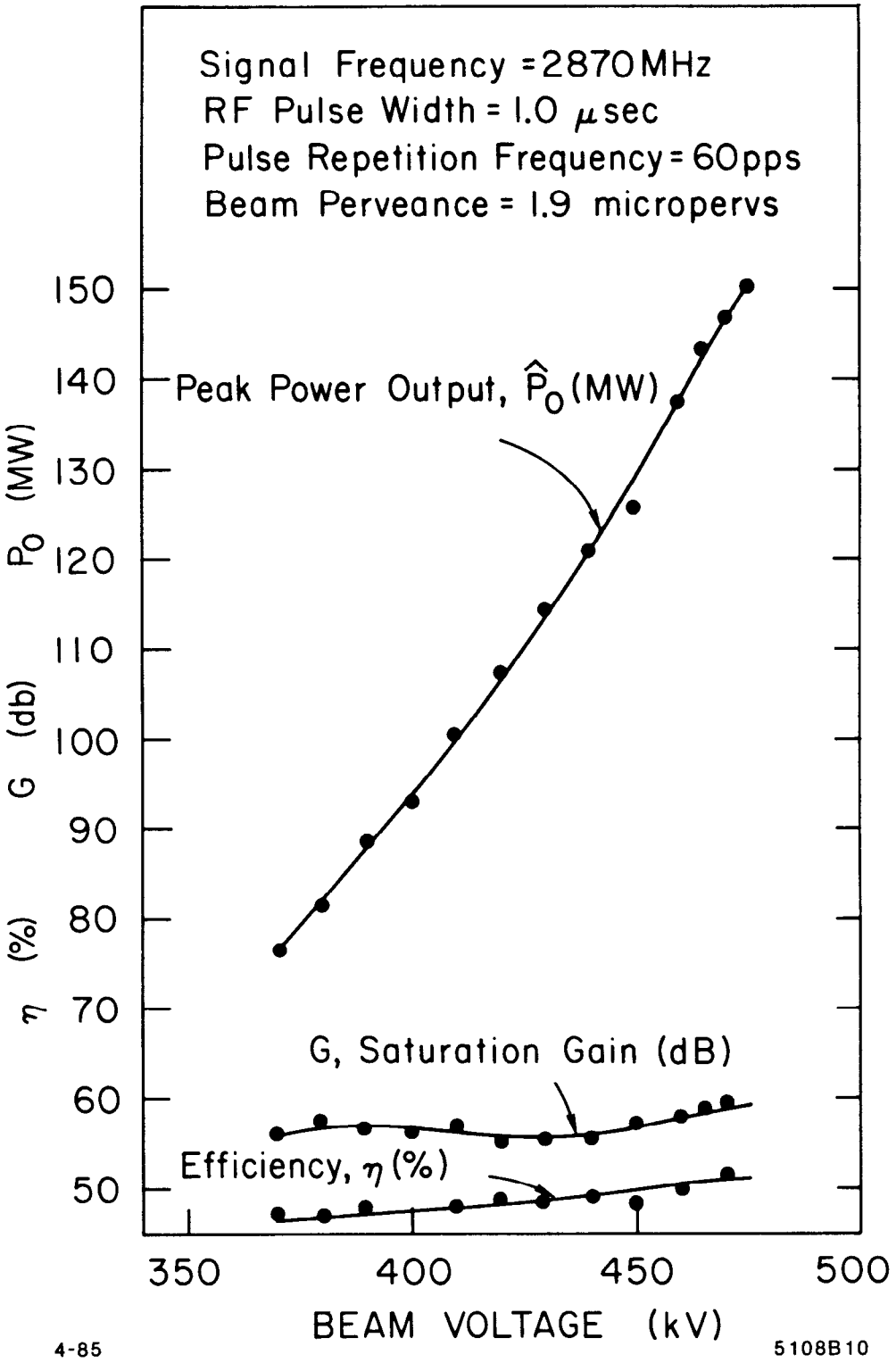
Signal Frequency = 2870 MHz
RF Pulse Width = 1.0 μsec
Pulse Repetition Frequency = 60pps
Beam Perveance = 1.9 micropervs
Peak Power Output, $\hat{P}_0$ (MW)
G, Saturation Gain (dB)
Efficiency, η (%)
P_0 (MW)
G (db)
η (%)
150
140
130
120
110
100
90
80
70
60
50
350
400
450
500
BEAM VOLTAGE (kV)
4-85
5108B10

Fig. 10

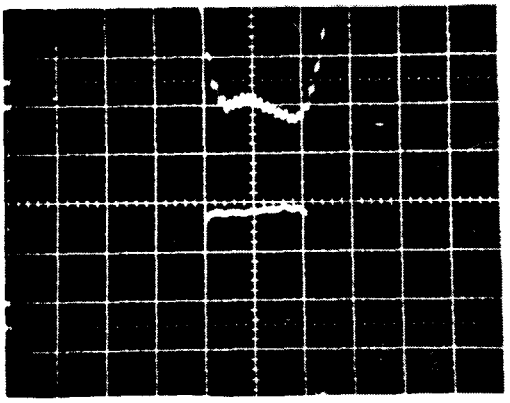

(a) 435 kV PRR = 60 pps

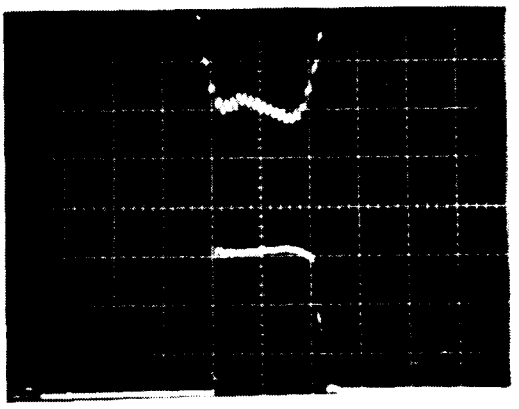

(b) 420 kV PPR = 120 pps

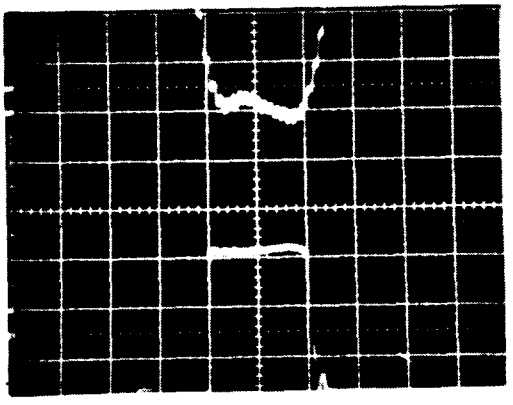

(c) 430 kV PRR = 120 pps

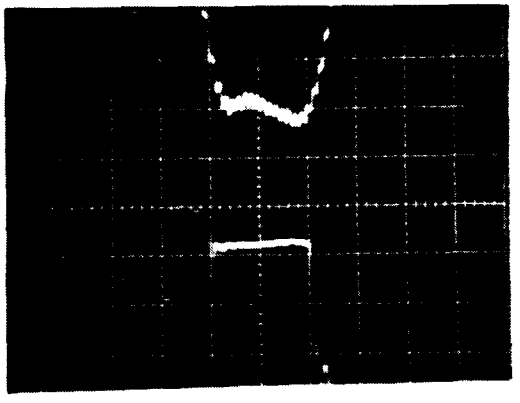

(d) 440 kV PRR = 120 pps

5108A11

5-85

Fig. 11

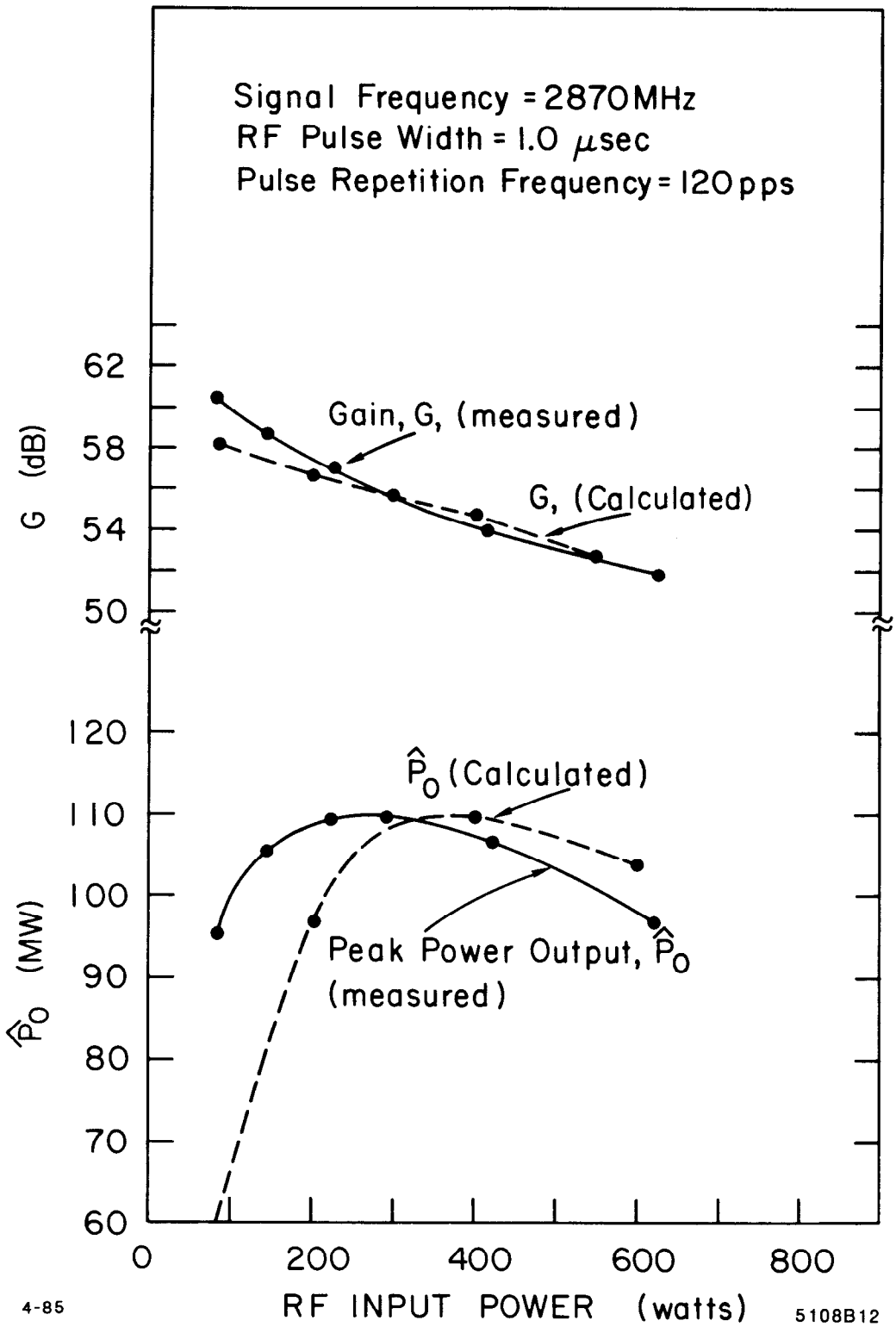
Signal Frequency = 2870MHz
RF Pulse Width = 1.0 μsec
Pulse Repetition Frequency = 120pps
G (dB)
62
58
54
50
Gain, G, (measured)
G, (Calculated)
$\hat{P}_o$ (MW)
120
110
100
90
80
70
60
$\hat{P}_o$ (Calculated)
Peak Power Output, $\hat{P}_o$
(measured)
0
200
400
600
800
RF INPUT POWER (watts)
4-85
5108B12

Fig. 12

(a)

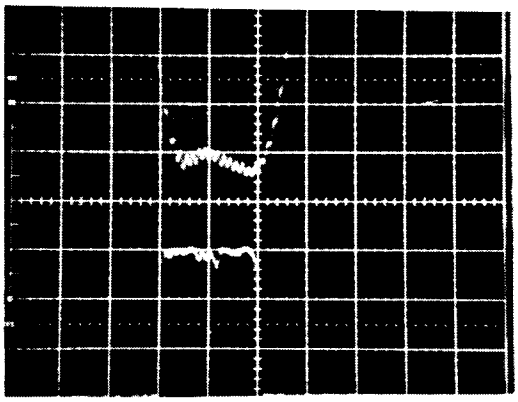

2 db
UNDER-DRIVEN

(b)

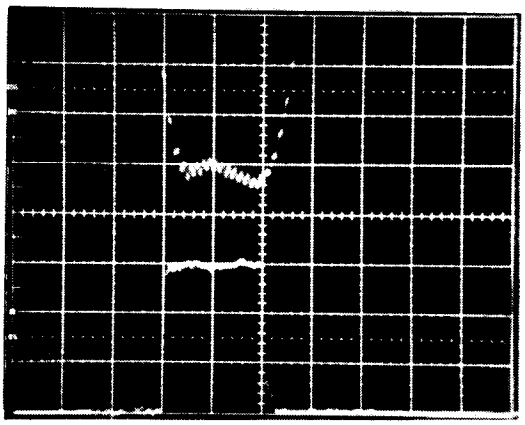

0-db
SATURATION

(c)

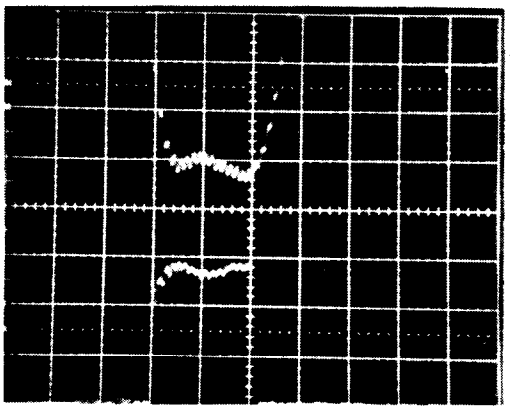

4.4 db
OVER-DRIVEN

4-85

5108A13

Fig. 13

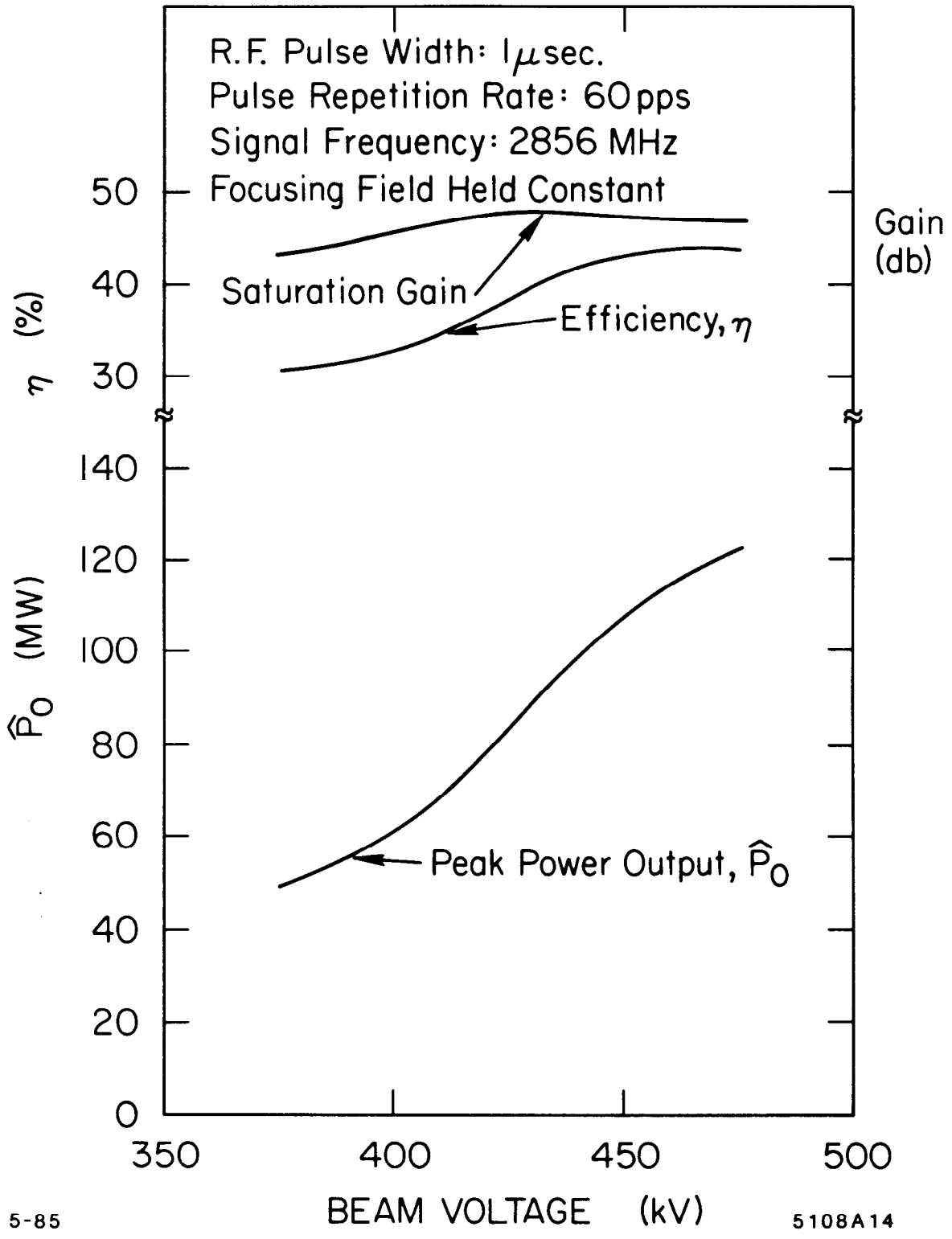
R.F. Pulse Width: 1μsec.
Pulse Repetition Rate: 60 pps
Signal Frequency: 2856 MHz
Focusing Field Held Constant
Saturation Gain
Efficiency, η
Peak Power Output, $\hat{P}_0$
η (%)
$\hat{P}_0$ (MW)
Gain (db)
BEAM VOLTAGE (kV)
0
20
40
60
80
100
120
140
30
40
50
350
400
450
500
5-85
5108A14

Fig. 14

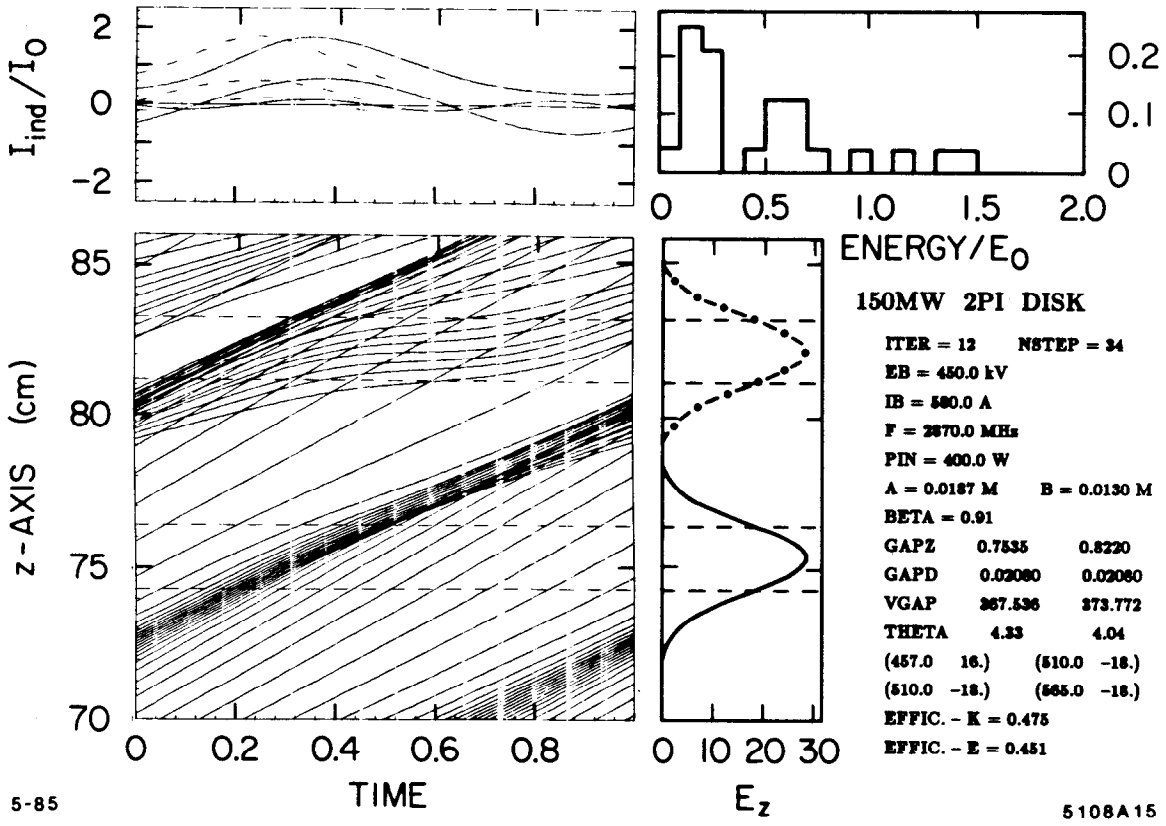
I_{ind}/I_0
2
0
-2
0.2
0.1
0
0
0.5
1.0
1.5
2.0
ENERGY/E_0
150MW 2PI DISK
ITER = 12 NSTEP = 34
EB = 450.0 kV
IB = 580.0 A
F = 2870.0 MHz
PIN = 400.0 W
A = 0.0187 M B = 0.0130 M
BETA = 0.91
GAPZ 0.7535 0.8220
GAPD 0.02080 0.02080
VGAP 367.536 373.772
THETA 4.33 4.04
(457.0 16.) (510.0 -16.)
(510.0 -16.) (565.0 -16.)
EFFIC. - K = 0.475
EFFIC. - E = 0.451
z-AXIS (cm)
85
80
75
70
0
0.2
0.4
0.6
0.8
TIME
0 10 20 30
E_z
5-85
5108A15

Fig. 15

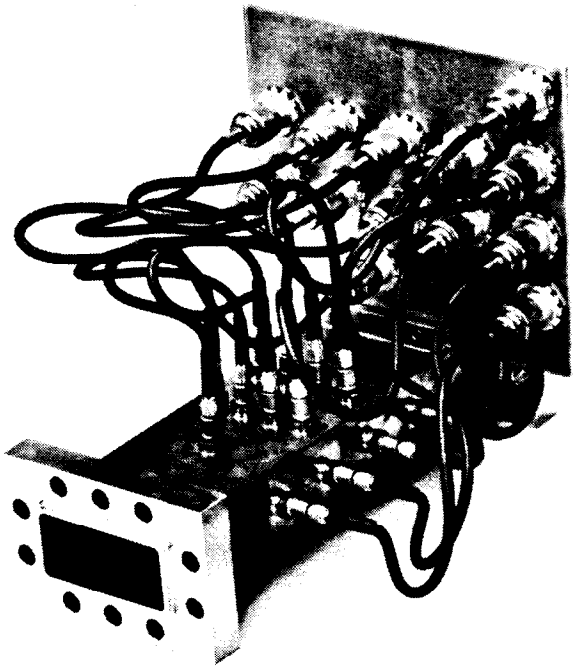

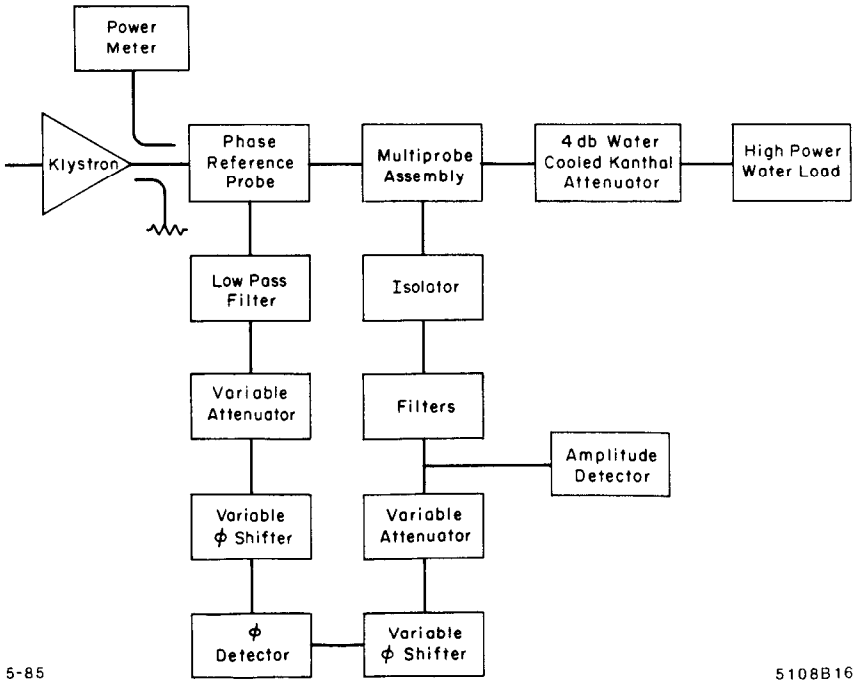
Power Meter
Klystron
Phase Reference Probe
Multiprobe Assembly
4 db Water Cooled Kanthal Attenuator
High Power Water Load
Low Pass Filter
Isolator
Variable Attenuator
Filters
Amplitude Detector
Variable ϕ Shifter
Variable Attenuator
ϕ Detector
Variable ϕ Shifter
5-85
5108B16

Fig. 16